Observed and calculated arching in the clayey silt of an earth dam

Reza Imam, Assistant Professor, & Nariman Mahabadi, MSc Student
Department of Civil and Environmental Engineering
Amirkabir University of Technology, Tehran, Iran

2011 Pan-Am CGS Geotechnical Conference

ABSTRACT
Arching in the core of earth dams may result from the partial transfer of weight of the more flexible, fine-grained core materials to the stiffer shell, filter, or abutment materials. This leads to a reduction in vertical stresses in the core, increasing the risk of hydraulic fracturing when the core is subjected to high water pressures during dam impoundment. In the current research, arching in the clayey silt core of a rockfill dam is examined based on both readings of dam instrumentation and finite element analyses of various dam sections. Since the wide rock valley of the dam varies substantially in depth and shape along the dam longitudinal section, arching occurs differently at the various sections. Effects of cross section shape and height on arching is examined, and differences between measured and calculated values are discussed with respect to the shape and height of the cross-sections analyzed.

RÉSUMÉ
Voilage dans le noyau des barrages en terre peuvent résulter de la cession partielle du poids de la plus souple, matériaux d'âme à grain fin à la plus rigide enveloppe, un filtre, ou des matériaux de butée. Cela conduit à une réduction des contraintes verticales dans le noyau, ce qui augmente le risque de fracturation hydraulique lorsque le noyau est soumis à des pressions hautes eaux pendant la mise en fourrière du barrage. Dans la recherche actuelle, des voûtes dans le noyau de limon argileux d'un barrage en enrochement est examinée en fonction des deux lectures de l'instrumentation du barrage et les analyses par éléments finis de sections différentes du barrage. Depuis la vallée du rock échelle du barrage varie considérablement en profondeur et la forme le long de la section longitudinale du barrage, des voûtes se produit différemment à différentes sections. Effets de la forme et la hauteur de coupe sur voûte est examiné, et les différences entre les valeurs mesurées et calculées sont discutées par rapport à la forme et la hauteur de la croix-sections analysées.

1 INTRODUCTION

1.1 General

In earth dams, arching may occur due to differential settlements between various parts of the dam, especially the central core and the shells or the dam abutments. As a result, the parts having higher vertical deformation transfer some of their weight to the stiffer parts. This load transfer leads to the development of shear stresses at the interfaces of the regions with different material properties, especially those with considerable contrast in deformability characteristics. Therefore, reductions in the amount of vertical and horizontal stresses at the lower parts of the core occur and this in turn, increases the chances of fracturing due to high water pressures applied to the core during dam impoundment. The more the core settles compared to the shell, the greater will be the shear stresses that develop at the interfaces. Eventually, while the exterior parts of the core may remain attached to the shell through shear stresses, separation of the upper section of the core from the lower section may occur (Shamsayi, 2004).

Upon application of hydraulic pressures, the aforementioned mechanisms can cause hydraulic fracturing and, eventually, piping in the dam core (Sharma, 1991). Some researchers even argue that using softer core materials which do not have enough shear strength which cause suspension of these materials on the shell might help decrease such risks (Knight et al., 1985).

1.2 The Doosti Dam

In the current research, arching in the clayey silt core of the Doosti dam in Northeastern Iran is examined based on both readings of dam instrumentation during construction, and finite element analysis of the various dam sections. The Doosti dam is an earth and rockfill dam with silty clay core, located on the common border of Iran and Turkmenistan at the north 35°75' latitude and east 61°9' longitude. The dam height above its rock foundation level is 79m at its deepest location; its crest length is 655m; and, the dam width is 428 m at foundation and 15 m at crest elevations. The dam cross-section and zoning are shown in Figure 1.

The dam primary purpose is to supply water for the city of Mashhad and for agriculture in the Sarakhs plain. The dam water storage volume is approximately 1.25 billion cubic meters. As shown in Figure 1, the impermeable part of the dam includes a silty clay core with a permeability of about $7.5*10^{-6}$cm/s, placed on the intact foundation bedrock. The average plasticity index (PI) of the material found locally for the dam core was approximately 4, making it necessary to take into account provisions

required in the design and construction of low-plasticity core dams.

In order to monitor the performance and behavior of the dam during its construction and long term utilization, a comprehensive instrumentation system consisting of various devices such as total pressure cells, electrical and other types of piezometers, inclinometers, etc. was designed and installed at various parts of the dam and its foundation.

The dam has a stiff rockfill shell and rock abutments and is, therefore, susceptible to arching and load transfer to both its shell and abutments. Since the wide dam valley varies substantially in depth and shape at various locations along the dam longitudinal section, arching may occur differently at various transverse dam sections. Figure 2 shows a plan of the dam layout and the locations of the six cross-sections at which numerical analyses were performed and instrumentation readings were examined.

In the current study, arching ratio, which is the ratio of the actual vertical stress to the theoretical gravitational stress expected due to weight of the overlying soil layers, was determined at various depths along the centerline of the core in selected transverse sections using finite element modeling. Vertical stresses obtained from dam instrumentations are then compared with those obtained from analysis, and possible causes of some observed differences between these values are discussed. Effects of cross section shape and height on the potential for arching is also examined.

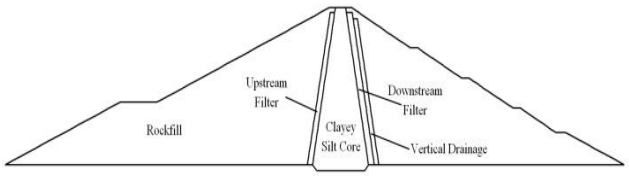

Figure 1. Typical cross section of the Doosti dam

2 NUMERICAL MODELLING

2.1 The Finite Element Model

In order to study the behavior of the Doosti dam during construction, six sections of the dam were modeled by a step by step application of the soil layers in each section. Construction of the dams was carried out at an average rate of 15 to 30 cm per day. However, in order to avoid excessive increases in numerical modeling efforts, larger layer thicknesses were used in the numerical modeling. In this respect, 2m thick layers were used for modeling the dam during construction. Due to the variable height of the dam at various sections, the number of layers was different, but the thickness of each layer was kept the same and equal to 2 meters in all the sections.

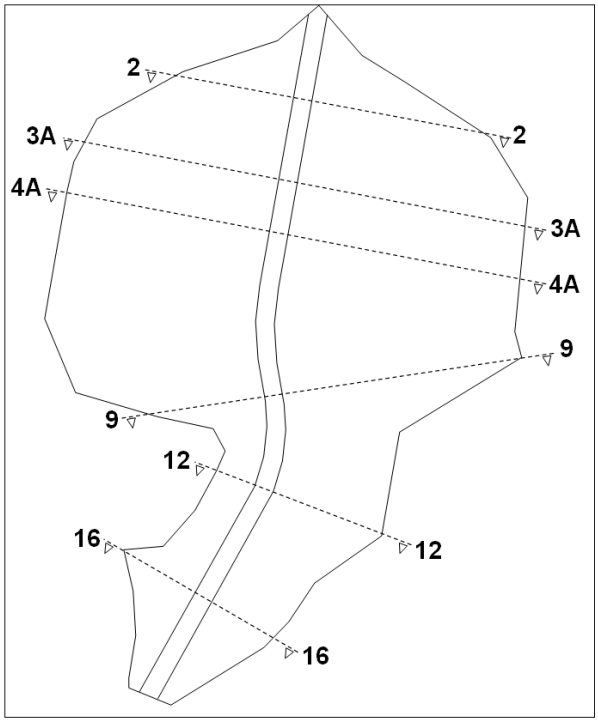

Figure 2. Layout of the Doosti dam and locations of the sections selected

Except for its initial parts, the Doosti dam was constructed at an approximately similar time rate. Therefore, in numerical modeling of the consolidation and time-dependent behavior of the dam, construction of each layer was assumed to be carried out at an average time of 15 days. Boundary conditions of the model such as geometrical conditions of the valley and the dam were modeled such that they correspond to the actual conditions, as much as possible. Also, mesh generation was performed automatically; and, due to the relatively complex geometries of the models, the meshing scheme was done using a combination of quadratic and triangular elements. Element dimensions were selected to be larger in the foundation and smaller in the areas near the dam body. Figure 3 presents the finite element models of the six sections of the dam selected for analysis and Table 1 provides a summary of specifications of these sections.

Table 1. Specifications of the selected cross sections

Section	Foundation elevation (m)	Crest elevation (m)	Number of construction stages	Construction time (day)
2-2	407	478	37	555
3A-3A	402	478	38	570
4A-4A	400	478	39	585
9-9	400	478	39	585
12-12	425	478	26	390
16-16	440	478	20	300

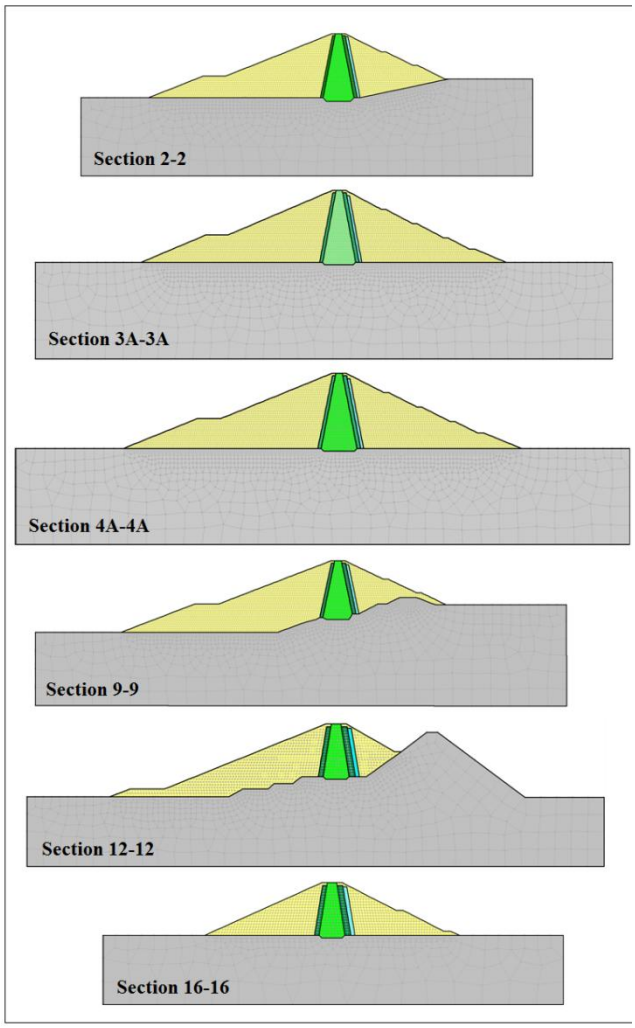

Figure 3. Finite element models of the dam cross-sections

2.2 Material Properties

Accuracy of prediction of earth dam deformations during construction is strongly dependent on the quality of representation of the stress-strain relationships of the dam materials. In rockfill dams, actual stress-strain behavior is controlled primarily by the properties of the rockfill which depends mainly on its intact strength, method of placement and particle size distribution after compaction. The embankment height is a significant factor as it determines the level of applied stresses within the embankment. Valley shape is also important in embankments constructed in narrow valleys due to the effects of cross-valley arching and the resultant reduction in applied stresses. Typical stress-strain relationships of rockfill materials obtained from field measurements during construction show that this relationship is generally non-linear, and has a general trend of decreasing secant (and tangent) modulus with increasing applied stress (Hunter and Fell, 2002).

Based on the above, the Duncan-Chang nonlinear hyperbolic constitutive model was used in the current finite element modeling. This model is widely applied in modeling soil behavior and is based on the shape of the stress-strain curve obtained from drained triaxial compression tests of both clay and sand, which can be approximated by a hyperbola with a reasonable degree of accuracy. Therefore, the stress-strain relationship of the soil is assumed to be nonlinear elastic, and the failure criterion is based on the Mohr-Coulomb two parameter model, with φ as the friction angle and c as the cohesion.

In the Duncan-Chang model, through using E_i and v_i as the initial tangent Young's modulus and tangent Poisson's ratio, the model describes the three important characteristics of soils: non-linearity, stress-dependency, and inelastic behavior. Both E_i and v_i are stress path dependent. At a given confining stress level, distinction is made between a primary loading stiffness, E_i and an unloading and reloading stiffness, E_{ur}.

The hyperbolic stress-strain curve is defined using the following equation for the stress-dependent elastic tangential modulus (E_t) at a given stress condition:

$$E_t = \left[1 - \frac{R_f(1-\sin\varphi)(\sigma_1-\sigma_3)}{2c\cos\varphi + 2\sigma_3\sin\varphi}\right]^2 K.P_a\left(\frac{\sigma_3}{P_a}\right)^n \quad [1]$$

in which σ_1 and σ_3 are the major and minor principal stresses, respectively; p_a is the atmospheric pressure; K is a modulus number, which is a dimensionless parameter representing Young's modulus; and, n is a modulus exponent, which governs the stress dependency of E_i on σ_3. The unloading and reloading behavior is defined using Eq. 2:

$$E_{ur} = K_{ur}P_a\left(\frac{\sigma_3}{P_a}\right)^n \quad [2]$$

in which K_{ur} is a modulus number similar to E_i but used for unloading and reloading, and other variables are as defined before.

The material properties used in Duncan-Chang modeling of the Doosti dam are presented in Table 2. Original material properties were estimated using results of laboratory triaxial, consolidation and direct shear tests. These properties were later adjusted based on back analyses of dam settlements recorded by inclinometers

installed at various locations within the dam core and shell (Mahabadi, 2011).

Table 2. Material properties used in numerical analyses

Zone	γ (ton/m^3)	K	K_{ur}	n	R_f	C (ton/m^2)	φ
Core	2.1	125	150	0.45	0.7	10	26
Filter	2.2	400	600	0.3	0.8	0	40
Rockfill	2.3	600	900	0.24	0.85	0	40

3 ANALYSIS RESULTS

3.1 Stresses and Strains

During the current study, several analyses for the determination of stresses and deformations in the dam body and clayey silt core were carried out. Contours of settlements and stresses were obtained for all the six sections shown in Figure 3. As an example, results obtained for the maximum section, Section 4A-4A are shown in Figure 4.

Figure 4(a) shows the calculated deformations at the end of construction. The figure shows that the maximum deformations occur at about the middle height of the core. Also, contours of vertical stresses and the occurrence of arching may be observed clearly in Figure 4(b), which shows that the vertical stresses in the core are smaller than those in the adjacent areas within the shell.

The pore water pressures developed at the end of construction are shown in Figure 4(c). These pore pressures are produced due to consolidation of the soils during construction and, as can be seen from the figure, are very small compared to the total vertical stresses developed in the core. The low plasticity, clayey silt core allows for a relatively rapid dissipation of the pore pressures developed during consolidation of the core. As a result, there is no significant difference between the effective and total vertical stresses developed in the dam at the end of construction.

3.2 Arching Ratios

The degree of arching in the core of earth and rockfill dams may be determined using the Arching Ratio (AR), which is defined at any point using the following relationship:

$$\text{Arching Ratio} = \frac{p}{\gamma h} \qquad [3]$$

in which p is the vertical stress measured by the total pressure cell at the current point, γ is the unit weight of soil and h is the height of soil above the current point. The AR is inversely proportional with the degree of arching. A lower AR is an indication of greater arching.

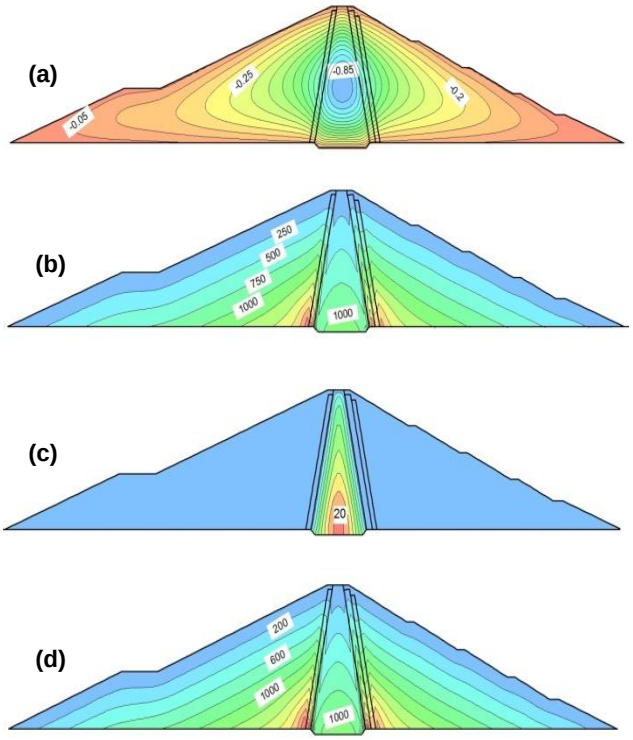

Figure 4. Contours obtained for section 4A-4A: (a) Total deformations (m) (b) Total vertical stresses (kPa) (c) Pore pressure (kPa) (d) Effective vertical stress (kPa)

Calculated variations of arching ratio with depth at the axis of the Doosti dam core are shown in Figure 5 for the six selected sections. A summary of the calculated maximum and minimum AR's at the end of construction is also shown in Table 3.

As can be seen from Figure 5, minimum arching ratios, which correspond to the maximum amount of arching, range from about 0.64 to 0.66 at the various cross sections. These arching ratios occur at approximately a quarter height of the dam from the foundation.

Table 3. Summary of the calculated arching ratios

Section	Minimum arching ratio		Maximum arching ratio	
	Quantity	Location	Quantity	Location
2-2	0.64	¼ H	0.97	Crest
3A-3A	0.66	¼ H	0.96	Crest
4A-4A	0.65	¼ H	0.97	Crest
9-9	0.66	¼ H	0.97	Crest
12-12	0.64	¼ H	0.90	Crest
16-16	0.64	¼ H	0.92	Crest

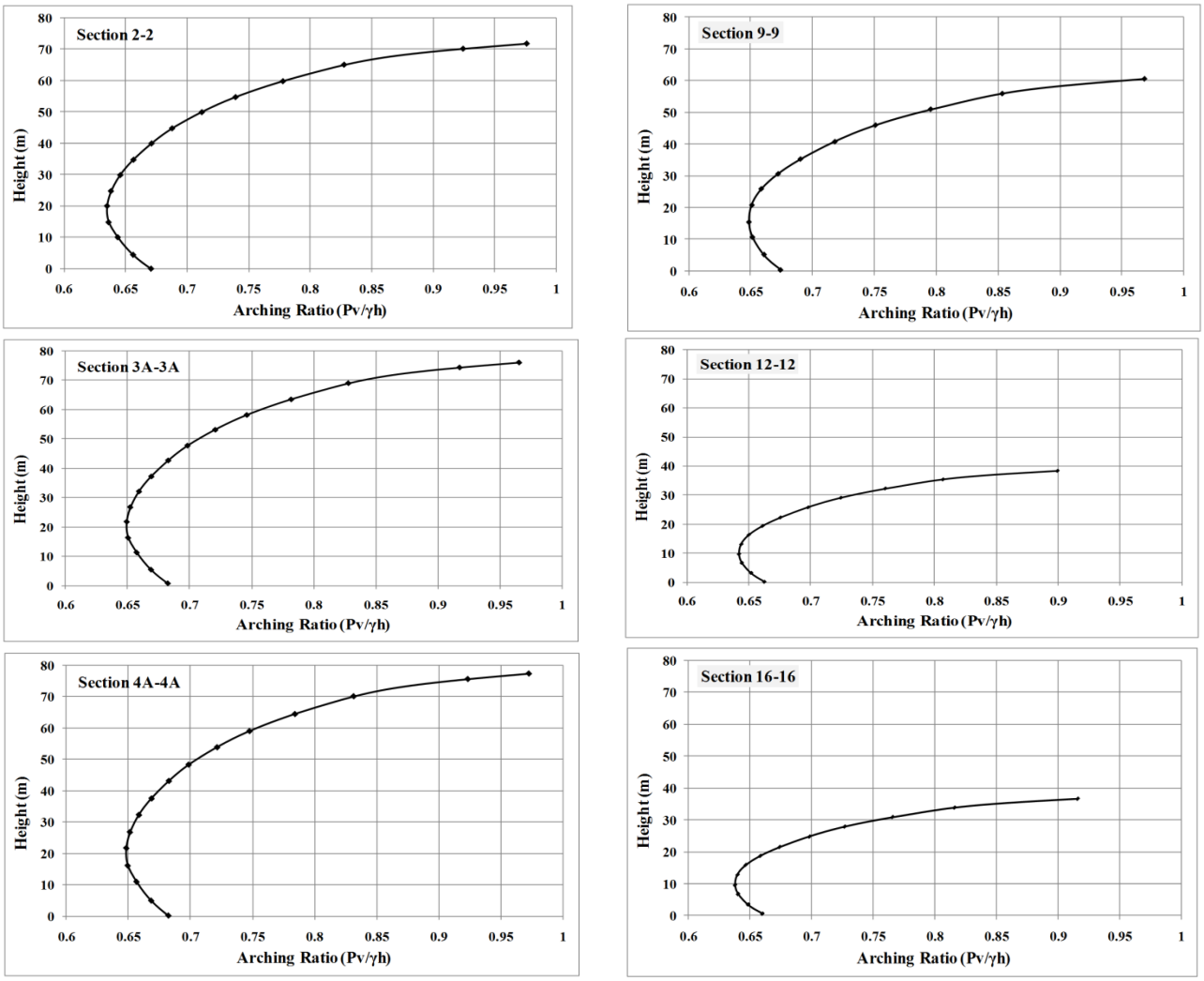

Figure 5. Calculated variations of arching ratio with depth at the axis of the Doosti Dam cross-sections

The lowest values of AR are obtained for sections 2-2, 12-12 and 16-16, in which the cross-sections have smaller widths and are supported by bedrock on their sides. As a result, more pronounced arching effects are observed in these sections. Compared to other sections, in these sections, AR's obtained in the dam crest are also lower, indicating more pronounced arching effects.

Calculated maximum arching ratios, which correspond to minimum arching effects, vary from 0.90 to 0.97 at the various cross-sections, and they occur at the dam crest in all the sections. Contact areas between the core and shell at elevations above the dam crest are not available and, as a result, shear stresses developed between the core and shell are smaller, resulting in less hanging of the core to the shell and less decrease in the vertical gravitational stresses in the core in these locations.

4 MEASURED AND CALCULATED ARCHING EFFECTS

In order to verify accuracy of the calculated vertical stresses and the corresponding calculated arching effects, results of the numerical analyses are compared with stresses measured by the total pressure cells installed in the core of the Doosti dam, as reported by Toosab Consulting Engineering Company (2005). The total pressure cells located in the largest section 4A-4A were damaged. Therefore, calculated and measured stresses are compared for cross sections 2-2, 3A-3A, 9-9, 12-12 and 16-16. Figure 6 shows locations of the total pressure cells installed in the aforementioned sections. The first number after the letters "TPC" refers to the section in which the cell is installed.

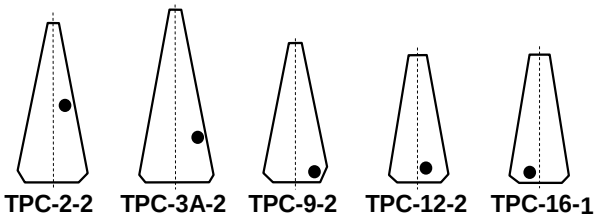

Figure 6. Locations of the total pressure cells installed in the dam core sections

Figure 7 shows comparisons between the observed and calculated total vertical stresses at the locations of the pressure cells. This figure indicates a good general agreement between results of the numerical analyses and readings of dam instrumentation. However, except for Section 16-16, in all other sections, measured stresses are somewhat higher than calculated stresses, indicating that actual arching effects are somewhat smaller compared to calculated effects in these sections.

Measured stresses indicate that arching effects are smaller in the wider sections 2-2, 3A-3A and 9-9 and higher in the narrower sections 12-12 and 16-16 such that in the latter section, measured stresses are considerably smaller than calculated stresses. It is noted that the calculated stresses are obtained from two-dimensional analyses of the dam sections, which do not consider the contributions of 3D effects to arching. It is likely that in the narrower sections and, particularly, in the narrow Section 16-16 closest to the dam abutment, some 3D effects lead to more pronounced arching and therefore, actual vertical stresses in the core are smaller than stresses obtained from 2D analysis of the dam section.

The degree of influence of arching depends also on the location of the point under consideration within the dam core, both laterally (i.e. how close it is relative to the shell/filter) as shown by Mahabadi (2011), and vertically, as shown in Figure 5. Figure 6 shows that the pressure cells are installed at various lateral and vertical locations. Some differences in the observed and calculated arching effects may be attributed to factors that have not been considered in the 2D numerical analyses of the dam sections. Table 4 compares the minimum arching ratios calculated and observed at the selected cross-sections.

Table 4. Comparison between calculated and observed minimum arching ratios at the end of construction

Instrument	Observed arching ratio	Calculated arching ratio
TPC-2-2	0.67	0.64
TPC-3A-2	0.67	0.61
TPC-9-2	0.50	0.46
TPC-12-2	0.66	0.66
TPC-16-1	0.54	0.65

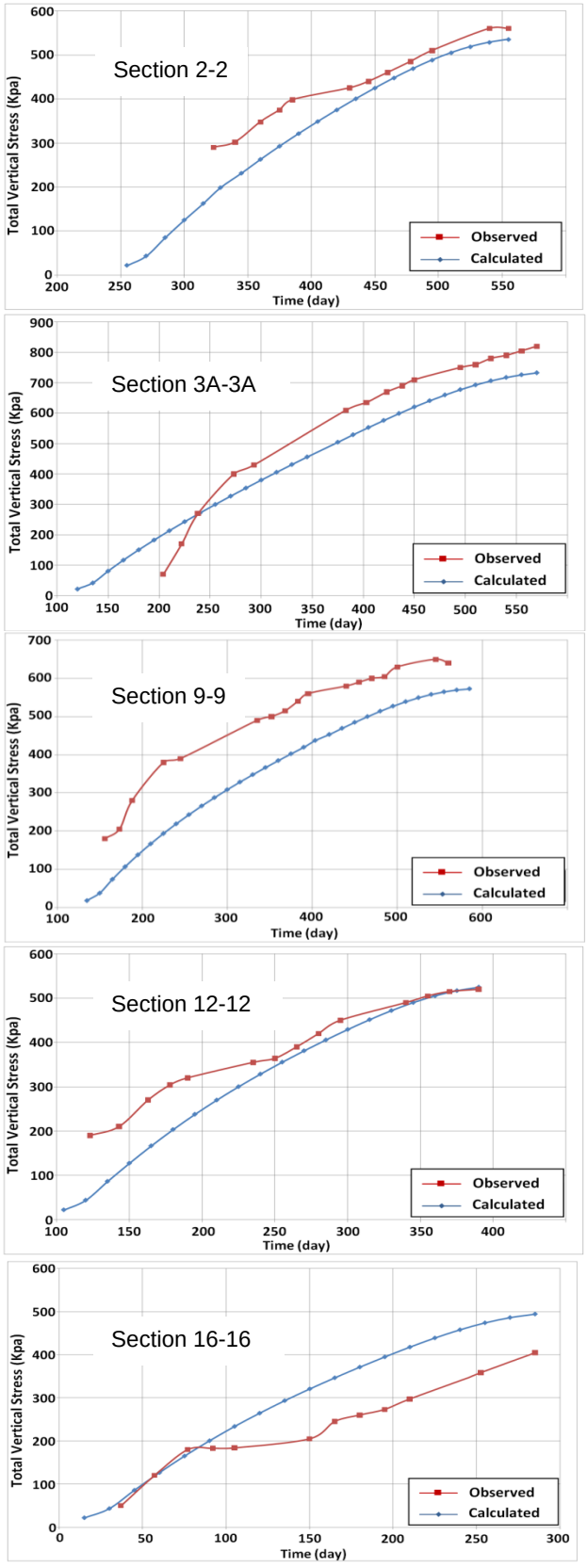

Figure 7. Total vertical stress in the core of dam sections

5- CONCLUSIONS

Finite element analysis of six transverse sections of the Doosti Dam showed that arching effects in the clayey silt core of the dam vary with elevation within the core, width of the section, and proximity of the rock abutments to the dam core. Highest arching effects were calculated at about one fourth of the dam height from the foundation, and lowest effects were calculated at the dam crest. Arching effects appear to be more pronounced at narrower sections and closer to the dam abutments where 3D effects are present.

Vertical stresses measured by pressure cells installed in the dam core at various sections and elevations were generally in good agreement with calculated stresses. Therefore, it may be concluded that two dimensional finite element modeling of the dam behavior using non-linear elastic constitutive modeling of the dam material provides a relatively good estimation of vertical stresses, including the effects of arching on these stresses. However, some 3D effects seemed to have influenced the measured stresses at some sections, but they could not be considered in the current 2D modeling. Except for the narrow section nearest to the dam abutment, arching effects obtained from measurements of total pressure cells were smaller than those obtained from the aforementioned calculations.

REFERENCES

Hunter, G. and Fell, R. 2002. The deformation behaviour of rockfill. UNICIV Report No. R-405, the University of New South Wales, School of Civil and Environmental Engineering.

Knight, D.J., Davis, P.D., Naylor, D.J. 1985, “Stress-strain behavior of the Monavasu soft core rockfill dam: prediction, performance and analysis", Proceeding of 15th. International Congress on Large Dams, Lausanne, 1985, 56, vol. I, PP. 1299-1326.

Mahabadi, N. 2011. *Analysis of the behavior of Doosti dam during construction and impounding and comparison with results of instrumentation.* MSc thesis, Amirkabir University of Technology. Tehran, Iran.

Shamsayi, A., 2004. *Design and construction of reservoir dams* (in Persian). Vol. 2, Science and Industry University Publication, Iran.

Sharma H.D. 1991. *Embankment Dams.* published by Raju Primlani for Oxford and IBH publishing co.

Toosab Consulting Engineering Company. 2005. *Third phase report of Doosti Storage Dam: Report of Dam monitoring to the end of construction*, Report No. 232093-2475-1, Mashad, Iran.